JACS
JOURNAL OF THE AMERICAN CHEMICAL SOCIETY
Communication
pubs.acs.org/JACS

Edge-to-Edge Oriented Self-Assembly of ReS_2 Nanoflakes

Qin Zhang,[†,§] Wenjie Wang,[†,§] Xin Kong,[†] Rafael G. Mendes,[‡] Liwen Fang,[†] Yinghui Xue,[†] Yao Xiao,[†] Mark H. Rümmeli,[‡,⊥,∥] Shengli Chen,[†] and Lei Fu*[,†]

[†]College of Chemistry and Molecular Science, Wuhan University, Wuhan 430072, China

[‡]IFW Dresden, P.O. Box 270116, 01069 Dresden, Germany

[⊥]College of Physics, Optoelectronics and Energy & Collaborative Innovation Center of Suzhou, Nano Science and Technology, Soochow University, Suzhou 215006, China

[∥]Centre of Polymer and Carbon Materials, Polish Academy of Sciences, M. Curie-Sklodowskiej 34, Zabrze 41-819, Poland

Supporting Information

ABSTRACT: The self-assembly of two-dimensional (2D) nanomaterials, an emerging research area, still remains largely unexplored. The strong interlayer attraction between 2D nanosheets leads to face-to-face stacking rather than edge-to-edge coupling. We demonstrate, for the first time, how one can induce and control an edge-to-edge self-assembly process for 2D nanomaterials. The extremely weak van der Waals coupling and strong anisotropy of ReS_2 allow us to realize an oriented self-assembly (OSA) process. The aspect ratio of the resulting ReS_2 nanoscrolls can be well controlled. In addition, we perform simulations to further explain and confirm the OSA process, demonstrating its great potential to be expanded as a general edge-to-edge self-assembly process suitable for other 2D nanomaterials.

Inspired by self-assembly phenomena in nature, such as that of the DNA double helix, researchers have made great efforts to assemble nanoscale building blocks into functional nanostructured materials over the past decades. Various strategies have been proposed and employed to fabricate highly ordered nanostructures via "self-correcting" assembly processes,[1] which have strongly promoted the rapid development of nanoscience and nanotechnology. Unfortunately, the self-assembly of two-dimensional (2D) nanomaterials still remains rarely explored, due to the strong interlayer coupling of the 2D nanosheets, which results in face-to-face stacking rather than an edge-to-edge geometry. For instance, driven by the strong van der Waals (vdW) forces, graphene sheets tend to aggregate and form graphite in order to minimize its surface free energy.[2] Undoubtedly, face-to-face stacking materials with poor surface area and kinetic ion transport cannot yield their ideal performance when they are utilized for energy storage and electrocatalysis. To avoid aggregation, it seems that 2D nanomaterials with weak interlayer coupling are required. Recent progress has shown that inherent anisotropy in crystalline structures,[3,4] as well as uniformity in size and shape,[5−8] can help scientists better understand the self-assembly mechanism.

As the top candidate for 2D semiconductor materials, transitional metal dichalcogenides (TMDs) have attracted the greatest attention in recent years. In the context of recent studies,[9,10] TMD nanostructures have significant potential in high-performance field-effect transistors, catalysis, and energy storage areas. Rhenium sulfide (ReS_2), an emerging member of the TMD family, can maximize and strengthen the weak interlayer coupling and the inherent anisotropy which also exist in most TMDs.[11] Due to an additional valence electron in rhenium, ReS_2 has layers that are extremely weakly vdW coupled to each other,[12] which allows two tangent ReS_2 nanoflakes to slide near without friction. Additionally, the anisotropic ratio of ReS_2 is larger than those of other reported 2D materials.[13] Moreover, the anisotropy of nanoflakes increases as the number of attached flakes increases.[3,14] The significant and inherent anisotropy of ReS_2 nanoflakes enables in-plane oriented self-assembly (OSA), so long as the relevant interlayer interactions are controlled. Data on the self-assembly of ReS_2 is scant, at best, but it is clearly a field worth exploiting.

Herein, we demonstrate, for the first time, the abnormal edge-to-edge self-assembly process of a 2D nanomaterial, namely ReS_2. The extremely weak vdW coupling and large anisotropy of ReS_2 allow us to realize an OSA process spanning the nanometer to micrometer range. Also, ReS_2 nanoflakes with the same size and shape tend to self-assemble in an edge-to-edge manner and eventually curl into micrometer-long nanoscrolls. We grow the ReS_2 nanowalls (ReS_2-NWs), in situ, on the surface of a three-dimensional graphene foam (3DGF). An electrochemical lithium intercalation process triggers the ReS_2-NWs to then exfoliate into nanoflakes. Scheme 1 demonstrates the formation process of ReS_2 nanoscrolls (ReS_2-NSs). Due to the competition between oriented attaching and self-rolling processes, we can tune which process dominates and regulate the aspect ratio of the resulting ReS_2-NSs. The controlled aspect ratio of such scrolls affords them greater potential in tuned electrical, mechanical, and thermal applications. We also conduct theoretical simulations to further explain and confirm the OSA process, demonstrating its potential as a technique for the self-assembly of other 2D nanomaterials.

3DGF is implemented as a binder-free current collector (Figure S1), over which ultra-uniform ReS_2-NWs grow in situ via chemical vapor deposition. As shown in the scanning

Received: June 20, 2016
Published: August 22, 2016

ACS Publications © 2016 American Chemical Society

DOI: 10.1021/jacs.6b06368
J. Am. Chem. Soc. 2016, 138, 11101−11104

Scheme 1. Schematic for the Process of Oriented Self-Assembly of ReS_2 Nanoscrolls

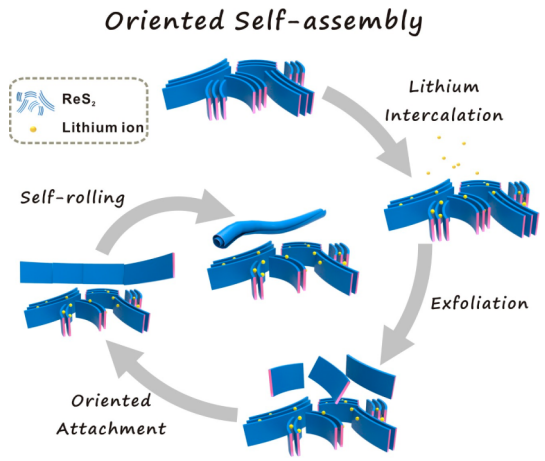

electron microscopy (SEM) images in Figure 1a,b, the nanowalls change into nanoscrolls upon lithium intercalation.

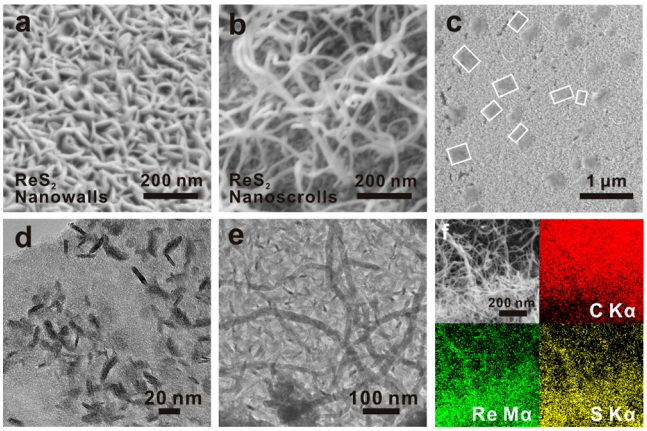

Figure 1. (a,d) SEM and TEM images of ReS_2-NWs uniformly deposited on 3DGF. (b,e) SEM and TEM images of ReS_2-NSs on 3DGF. (c) SEM image of rectangular ReS_2 nanoflakes in the intermediate phase. (f) SEM observation and the corresponding EDX elemental mapping of carbon, sulfur, and rhenium.

During this process, large amounts of nanoflakes form and approach others (Figure 1c). Due to the strong anisotropic dipole−dipole interactions,[15,16] these nanoflakes are more inclined to form rectangles with a preferred growth direction. Figure S2 shows the uniformity and high yield of nanoscrolls formed through this OSA technique. Transmission electron microscopy (TEM) images provide greater details about the structures of the ReS_2-NWs and ReS_2-NSs (Figure 1d,e). The average length of ReS_2-NWs is ∼20−30 nm (Figure S3), which is far less than that of the ReS_2-NSs (>1 μm). To form such a 1 μm nanoscroll, more than 50 individual nanowalls must be exfoliated and assembled, with each flake attaching along an exact axis. Thus, it is clear that the formation of nanoscrolls must be an edge-to-edge self-assembly process. The typical energy-dispersive X-ray spectroscopic (EDX) map (Figure 1f) shows that the sulfur elemental map overlaps with that of rhenium, complementing well with the carbon elemental map which arises from the 3DGF support. The EDX analysis indicates a homogeneous distribution of Re and S in the nanoscroll structure.

To better understand the composition of the nanoscrolls, we compared various characterizations of both the ReS_2-NWs and ReS_2-NSs (Figure S4). In Figure S4a, X-ray diffraction (XRD) measurements demonstrate the characteristic diffraction peaks belonging to graphene (JCPDS No. 41-1487). Two distinct (001) and (201) reflections are observed from the ReS_2-NWs (JCPDS No. 89-0341). For the nanoscrolls, the (001) diffraction peak weakens and the (201) diffraction peak disappears. This transformation is due to a decrease of the (001) facets when the sheets curl into NSs and the attachment occurring along the (201) facets. The Raman spectra in Figure S4b show that both of them have a distinct peak at 162 cm^{-1}, corresponding to the in-plane (E_{2g}) vibrational modes of ReS_2.[12,17,18] The data analysis shows a minor blue shift of the A_{1g} peak from 208 to 210 cm^{-1} with reduced peak relative intensity, due to the scrolling of ReS_2. Owing to suppression of interlayer coupling and strain from curvature in the nanoscrolls, atom vibration is altered significantly.[19,20] Figure S4c,d demonstrate the X-ray photoelectron spectroscopy (XPS) analysis of the elemental composition of the ReS_2-NSs on 3DGF. Three major peaks correspond to the C 1s, Re 4f, and S 2p states. The ratio of Re:S is approximately 1:2 atom%, which is in good agreement with the stoichiometric value for ReS_2. Figure S4d, left side, shows the core 4f 7/2 and 4f 5/2 level peaks for rhenium located at ∼41.95 and 44.36 eV.[12] Figure S4d, right side, shows two peaks at 162.4 and 163.2 eV, corresponding to the S 2p 3/2 and S 2p 1/2 states.

In order to further confirm the exact structure of ReS_2-NSs, high-resolution TEM (HR-TEM) studies are conducted (Figure 2). We investigate the morphology of a nanoscroll

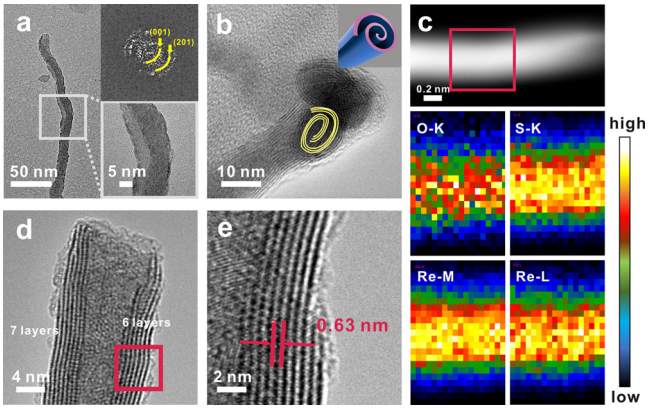

Figure 2. TEM characterization of the ReS_2-NSs. (a) TEM characterization and corresponding FFT pattern (inset). (b) HR-TEM image from the profile of nanoscroll and 3D models (inset). Yellow helix represents anticlockwise rotation. (c) TEM image and the EDX mapping of O-K, S-K, Re-M, and Re-L, respectively. The red square on the TEM image highlights the area of EDX mapping. (d,e) HR-TEM images of the edge of a nanoscroll.

(Figure 2a), presenting the edge with a clearly distinct contrast (inset in Figure 2a, bottom). This appears to be the opening of the nanoscroll, before it completely rolled up. Moreover, the fast Fourier transform (FFT; inset in Figure 2a, top) clearly demonstrates that there are two diffuse diffraction rings, corresponding to the (001) and (201) facets of ReS_2. Figure 2b presents the cross-section of a nanoscroll as well as a 3D schematic (inset), revealing its obvious anticlockwise curling direction (Figure S5). Figure 2c shows the local dispersive EDX elemental mapping data, demonstrating the uniform distribu-

DOI: 10.1021/jacs.6b06368
J. Am. Chem. Soc. 2016, 138, 11101−11104

tion of S and Re in the nanoscroll, with a Re:S ratio of approximately 1:2 (Figure S6). Figure 2d presents a clear image of nanoscroll opening with unequal layers on both sides, illustrating that it is a nanoscroll rather than a nanotube. By magnifying the edge (red square), one can determine the interlayer distance to be 0.63 nm (Figure 2e), which fits with that of fullerene-like ReS_2,[21] indicating no contamination between the stacked ReS_2 layers[22−24] in the nanoscroll. As shown in Figure S7, a typical attachment or anchor point was found along the nanoscroll. To provide insight into the orientation, FFT diffractograms were obtained and displayed the same crystal orientation above and below the attachment point. This indicates that the attached section is oriented with respect to the scroll.

To better understand the OSA process, we consider how the layers slide and observe the nanoscrolls with fishbone-like openings (Figure 3a−c). Since the curling speed is faster than

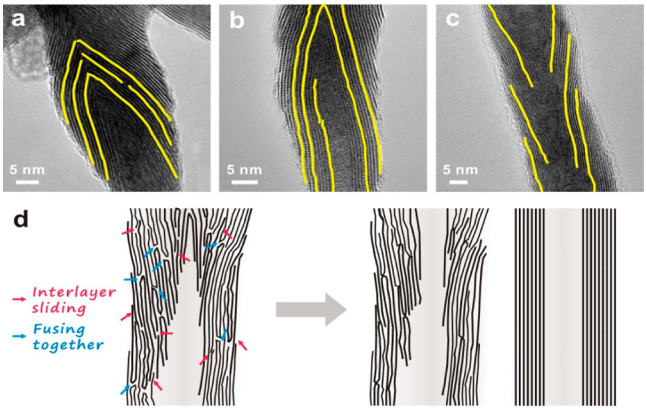

Figure 3. (a−c) TEM images of the fishbone-like openings. (d) Simulation of the "self-correcting" process.

their attachment,[25] adjacent nanoflakes take the lead in twisting along the pre-existing nanoscrolls and then gradually "self-correct". From the abutment fishbone-like structure to the almost paralleled nanoscroll, interlayer sliding can help sections of sheets to eventually fuse together. Only when structurally analogous surfaces of these sections approach each other can they be driven to generate chemical bonds between Re and S atoms of opposite edges so as to realize full coordination.[26] As illustrated in Figure 3d, the fishbone-like structure undergoes interlayer sliding, which allows sections to align and fuse together at common edges. Due to the structural anisotropy and Li insertion,[27,28] the interlayer friction force is very low, further facilitating the sliding of the ReS_2 sheets.

At the beginning of lithiation, the Li ions insert into interlayer of ReS_2-NWs, thus expanding the interlayer distance. Since the Li ions are more inclined to adsorb along the Re−Re chain,[18] the long-range Coulombic repulsive interaction between S layers in different ReS_2 lamellas is strengthened.[27] Subsequently, the nanoflakes can follow one of three possible routes (Figure 4): In Route 1, the adjacent ReS_2 nanoflakes stack face-to-face, with a coupling energy of ∼18 meV per unit cell.[17] This extremely weak coupling seems to be insufficient to overcome the continuous impact of Li ions. In Route 2, randomly distributed nanoflakes retain their disordered structure. Since the repulsive interaction increases with growing number of Li ions, the random distribution of ReS_2 nanoflakes cannot be sustained any more. In Route 3, the pre-existing

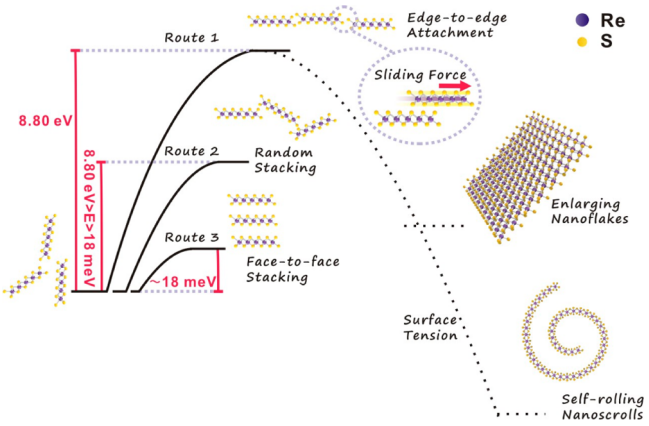

Figure 4. Simulated calculation and comparison of the edge-to-edge OSA process.

nanoflakes approach in the same orientation, driven by the long-distance anisotropic force.[16] Affected by the combination of anisotropic and electrostatic forces, these nanoflakes tend to slide away.[20] Since the Coulombic repulsive interaction is strongly influenced by the electronic states,[25] the electrical charges of the lithium ions would further increase the sliding force. Meanwhile, the ReS_2 nanoflakes with coherent facets approach and then fuse together. Due to the reduction in surface area and surface energy, the original exposed facets of both nanoflakes disappear. To further confirm the attaching facets, we also simulated the binding energies between different facets of ReS_2 nanoflakes (Figure S8). With appropriate calculations, the binding energy of the [010] direction is 8.80 eV, while that of the [100] direction is 2.99 eV. With the same number of Re−S bonds, the (201) facet is analogous to the [010] direction, which means ReS_2 nanoflakes prefer to attach along the (201) facet. Subsequent attaching and self-rolling process will dramatically reduce the total energy, indeed far less than that for Route 1.

Thereafter, the continued growth of ReS_2 nanoflakes can be considered as an avalanche-like process driven by the increasing anisotropy and the dipole moment as the number of attached nanoflakes increases.[14] The amount of exfoliated nanoflakes is increased by lowering the discharge voltage in the liquid electrolyte system, providing more opportunities for oriented attachment. Since the twisting time is directly proportional to the concentration,[25] the rate of self-rolling will be restrained once the equilibrium is achieved. For nanoflakes, the curling time is many orders of magnitude shorter than the time of the attachment process.[25] When the pre-existing ReS_2 nanoflakes are limited, it is easier to twist instead of connecting. When it comes to the maximum amount of nanoflakes, the attachment dominates, thereby lengthening the nanoscrolls. Moreover, we further demonstrate this competition between attaching and self-rolling by comparing the morphologies of the nanoscrolls under different discharge voltages (Figure S9). The decomposition of ReS_2 and formation of Re and Li_2S occurs with excess Li insertion[29,30] (Figure S10). Hence, by lowering the discharge voltage, the aspect ratio of nanoscroll can be continuously tuned.[30]

In summary, for the first time we demonstrate a scale-controlled oriented self-assembly process of a two-dimensional nanomaterial. By means of this technique, we also first realize the transformation of transitional metal dichalcogenide nanosheets into nanoscrolls, triggered by an electrochemical

DOI: 10.1021/jacs.6b06368
J. Am. Chem. Soc. 2016, 138, 11101−11104

lithiation process. The ReS_2 nanoflakes of similar size and shape tend to edge-to-edge self-assemble due to the extremely weak van der Waals coupling and in-plane anisotropy. For the purpose of minimizing the surface energy, the growing ReS_2 nanoflakes are compelled to roll up. By tuning the discharge voltage, we can also regulate the aspect ratio of the nanoscrolls. With exhaustive characterizations and simulations, we confirm the mechanism of the OSA process and the morphology of nanoscrolls. We believe that this method can also be expanded to the edge-to-edge OSA of other 2D nanomaterials.

■ ASSOCIATED CONTENT

Supporting Information

The Supporting Information is available free of charge on the ACS Publications website at DOI: 10.1021/jacs.6b06368.

Experimental details and supplementary Figures S1−S10 (PDF)

■ AUTHOR INFORMATION

Corresponding Author

*leifu@whu.edu.cn

Author Contributions

[§]Q.Z. and W.W. contributed equally to this work.

Notes

The authors declare no competing financial interest.

■ ACKNOWLEDGMENTS

The research was supported by the Natural Science Foundation of China (Grants 51322209, 21473124) and the Sino-German Center for Research Promotion (Grants GZ 871). We thank Prof. Xinping Ai for characterizations.

■ REFERENCES

(1) Baek, K.; Hwang, I.; Roy, I.; Shetty, D.; Kim, K. *Acc. Chem. Res.* **2015**, *48*, 2221.

(2) Cote, L. J.; Kim, F.; Huang, J. *J. Am. Chem. Soc.* **2009**, *131*, 1043.

(3) Cho, K. S.; Talapin, D. V.; Gaschler, W.; Murray, C. B. *J. Am. Chem. Soc.* **2005**, *127*, 7140.

(4) Sinyagin, A. Y.; Belov, A.; Tang, Z.; Kotov, N. A. *J. Phys. Chem. B* **2006**, *110*, 7500.

(5) Rogach, A. L.; Talapin, D. V.; Shevchenko, E. V.; Kornowski, A.; Haase, M.; Weller, H. *Adv. Funct. Mater.* **2002**, *12*, 653.

(6) Murray, C. B.; Sun, S. H.; Gaschler, W.; Doyle, H.; Betley, T. A.; Kagan, C. R. *IBM J. Res. Dev.* **2001**, *45*, 47.

(7) Wang, X.; Zhuang, J.; Peng, Q.; Li, Y. *Nature* **2005**, *437*, 121.

(8) Park, J.; Joo, J.; Kwon, S. G.; Jang, Y.; Hyeon, T. *Angew. Chem., Int. Ed.* **2007**, *46*, 4630.

(9) Pradhan, N. R.; McCreary, A.; Rhodes, D.; Lu, Z.; Feng, S.; Manousakis, E.; Smirnov, D.; Namburu, R.; Dubey, M.; Walker, A. R. H.; Terrones, H.; Terrones, M.; Dobrosavljevic, V.; Balicas, L. *Nano Lett.* **2015**, *15*, 8377.

(10) Xu, K.; Deng, H. X.; Wang, Z.; Huang, Y.; Wang, F.; Li, S. S.; Luo, J. W.; He, J. *Nanoscale* **2015**, *7*, 15757.

(11) Lorchat, E.; Froehlicher, G.; Berciaud, S. *ACS Nano* **2016**, *10*, 2752.

(12) Keyshar, K.; Gong, Y.; Ye, G.; Brunetto, G.; Zhou, W.; Cole, D. P.; Hackenberg, K.; He, Y.; Machado, L.; Kabbani, M.; Hart, A. H.; Li, B.; Galvao, D. S.; George, A.; Vajtai, R.; Tiwary, C. S.; Ajayan, P. M. *Adv. Mater.* **2015**, *27*, 4640.

(13) Liu, E.; Fu, Y.; Wang, Y.; Feng, Y.; Liu, H.; Wan, X.; Zhou, W.; Wang, B.; Shao, L.; Ho, C. H.; Huang, Y. S.; Cao, Z.; Wang, L.; Li, A.; Zeng, J.; Song, F.; Wang, X.; Shi, Y.; Yuan, H.; Hwang, H. Y.; Cui, Y.; Miao, F.; Xing, D. *Nat. Commun.* **2015**, *6*, 6991.

(14) Hu, T.; Gao, Y.; Wang, Z. L.; Tang, Z. Y. *Front. Phys. China* **2009**, *4*, 487.

(15) Lu, C.; Tang, Z. *Adv. Mater.* **2016**, *28*, 1096.

(16) Wang, P. P.; Sun, H.; Ji, Y.; Li, W.; Wang, X. *Adv. Mater.* **2014**, *26*, 964.

(17) Tongay, S.; Sahin, H.; Ko, C.; Luce, A.; Fan, W.; Liu, K.; Zhou, J.; Huang, Y. S.; Ho, C. H.; Yan, J.; Ogletree, D. F.; Aloni, S.; Ji, J.; Li, S.; Li, J.; Peeters, F. M.; Wu, J. *Nat. Commun.* **2014**, *5*, 3252.

(18) Zhang, Q.; Tan, S.; Mendes, R. G.; Sun, Z.; Chen, Y.; Kong, X.; Xue, Y.; Rummeli, M. H.; Wu, X.; Chen, S.; Fu, L. *Adv. Mater.* **2016**, *28*, 2616.

(19) Hershfinkel, M.; Gheber, L. A.; Volterra, V.; Hutchison, J. L.; Margulis, L.; Tenne, R. *J. Am. Chem. Soc.* **1994**, *116*, 1914.

(20) Rice, C.; Young, R. J.; Zan, R.; Bangert, U.; Wolverson, D.; Georgiou, T.; Jalil, R.; Novoselov, K. S. *Phys. Rev. B: Condens. Matter Mater. Phys.* **2013**, *87*, 081307.

(21) Yella, A.; Therese, H. A.; Zink, N.; Panthöfer, M.; Tremel, W. *Chem. Mater.* **2008**, *20*, 3587.

(22) Xie, X.; Ju, L.; Feng, X.; Sun, Y.; Zhou, R.; Liu, K.; Fan, S.; Li, Q.; Jiang, K. *Nano Lett.* **2009**, *9*, 2565.

(23) Zhu, Y. Q.; Hsu, W. K.; Terrones, H.; Grobert, N.; Chang, B. H.; Terrones, M.; Wei, B. Q.; Kroto, H. W.; Walton, D. R. M.; Boothroyd, C. B.; Kinloch, I.; Chen, G. Z.; Windle, A. H.; Fray, D. J. *J. Mater. Chem.* **2000**, *10*, 2570.

(24) Zhu, Y. Q.; Sekine, T.; Brigatti, K. S.; Firth, S.; Tenne, R.; Rosentsveig, R.; Kroto, H. W.; Walton, D. R. *J. Am. Chem. Soc.* **2003**, *125*, 1329.

(25) Chivilikhin, S. A.; Popov, I. Y.; Blinova, I. V.; Kirillova, S. A.; Konovalov, A. S.; Oblogin, S. I.; Tishkin, V. O.; Chernov, I. A.; Gusarov, V. V. *Glass Phys. Chem.* **2007**, *33*, 315.

(26) Penn, R. L.; Banfield, J. F. *Science* **1998**, *281*, 969.

(27) Onodera, T.; Morita, Y.; Nagumo, R.; Miura, R.; Suzuki, A.; Tsuboi, H.; Hatakeyama, N.; Endou, A.; Takaba, H.; Dassenoy, F.; Minfray, C.; Joly-Pottuz, L.; Kubo, M.; Martin, J. M.; Miyamoto, A. *J. Phys. Chem. B* **2010**, *114*, 15832.

(28) Martin, J. M.; Donnet, C.; Le Mogne, T.; Epicier, T. *Phys. Rev. B: Condens. Matter Mater. Phys.* **1993**, *48*, 10583.

(29) Zeng, Z.; Yin, Z.; Huang, X.; Li, H.; He, Q.; Lu, G.; Boey, F.; Zhang, H. *Angew. Chem., Int. Ed.* **2011**, *50*, 11093.

(30) Wang, H.; Lu, Z.; Xu, S.; Kong, D.; Cha, J. J.; Zheng, G.; Hsu, P. C.; Yan, K.; Bradshaw, D.; Prinz, F. B.; Cui, Y. *Proc. Natl. Acad. Sci. U. S. A.* **2013**, *110*, 19701.

■ NOTE ADDED AFTER ASAP PUBLICATION

This paper was published on August 25, 2016 and was partially corrected; the fully corrected version was reposted on September 7, 2016.

■ NOTE ADDED AFTER ISSUE PUBLICATION

Due to a production error, Figure 2 was published incorrectly; the correct version was reposted on September 9, 2016.

DOI: 10.1021/jacs.6b06368
J. Am. Chem. Soc. 2016, 138, 11101−11104